AIP | Review of Scientific Instruments

Intensity correlation measurement system by picosecond single shot soft x-ray laser

Maki Kishimoto, Kazumichi Namikawa, Kouta Sukegawa, Hiroshi Yamatani, Noboru Hasegawa, and Momoko Tanaka

Citation: Review of Scientific Instruments **81**, 013905 (2010); doi: 10.1063/1.3280173
View online: http://dx.doi.org/10.1063/1.3280173
View Table of Contents: http://scitation.aip.org/content/aip/journal/rsi/81/1?ver=pdfcov
Published by the AIP Publishing

Intensity correlation measurement system by picosecond single shot soft x-ray laser

Maki Kishimoto,[1,2] Kazumichi Namikawa,[1,2,3] Kouta Sukegawa,[1] Hiroshi Yamatani,[1] Noboru Hasegawa,[1] and Momoko Tanaka[1,2]
[1]*Quantum Beam Science Directorate, Japan Atomic Energy Agency, Kizugawa, Kyoto 619-0215, Japan*
[2]*Japan Science and Technology Agency, CREST, Chiyoda, Tokyo 102-0075, Japan*
[3]*Department of Physics, Tokyo Gakugei University, Koganei, Tokyo 184-8501, Japan*

(Received 18 September 2009; accepted 8 December 2009; published online 19 January 2010)

We developed a new soft x-ray speckle intensity correlation spectroscopy system by use of a single shot high brilliant plasma soft x-ray laser. The plasma soft x-ray laser is characterized by several picoseconds in pulse width, more than 90% special coherence, and 10^{11} soft x-ray photons within a single pulse. We developed a Michelson type delay pulse generator using a soft x-ray beam splitter to measure the intensity correlation of x-ray speckles from materials and succeeded in generating double coherent x-ray pulses with picosecond delay times. Moreover, we employed a high-speed soft x-ray streak camera for the picosecond time-resolved measurement of x-ray speckles caused by double coherent x-ray pulse illumination. We performed the x-ray speckle intensity correlation measurements for probing the relaxation phenomena of polarizations in polarization clusters in the paraelectric phase of the ferroelectric material $BaTiO_3$ near its Curie temperature and verified its performance. © *2010 American Institute of Physics.* [doi:10.1063/1.3280173]

I. INTRODUCTION

The observation of the fluctuation in nanometer region so far has been performed by use of synchrotron radiation.[1–5] However, even in the case of using third generation high brilliant synchrotron radiation, it has taken from several tens of microseconds to a few seconds in order to execute an intensity correlation measurement because the fraction of coherent photons in its total photon flux is only about 0.1%. Therefore, the intensity correlation measurements performed so far have been restricted to slow phenomena such as macroscopic fluctuation in order-disorder structure alloys,[6] diffusion process in Brownian motion in colloidal solutions,[7] antiferromagnetic domain fluctuations,[5] and so on, and it had been hard to probe fast phenomena in the picosecond time range such as thermal relaxation of materials.

A plasma soft x-ray laser (SXRL) using the transient collisional excitation scheme and a double-target configuration is a single shot soft x-ray source, having picosecond pulse width, and x-ray photons within one SXRL pulse corresponds to 1 s accumulation of synchrotron radiation beam.[8] Moreover, more than 90% of x-ray photons in the SXRL pulse are coherent.[9] However, the electronic correlation measuring system commonly used in synchrotron radiation experiments cannot be applied to the intensity correlation measurement by such as the single shot SXRL.

We have developed a new apparatus for generating double pulses of the high coherent SXRL, and we have developed an x-ray speckle intensity correlation spectroscopy system for direct observation of dynamic processes of material in the picosecond time scale using a double coherent pulse illumination technique. We confirmed the performance of this system by observing the picosecond relaxation time of dipole moments in the polarization clusters in the ferroelectric material $BaTiO_3$ in the vicinity of its Curie temperature.

II. INSTRUMENTATION

The soft x-ray speckle intensity correlation spectroscopy system has been installed in the plasma x-ray laser facility at Japan Atomic Energy Agency.[10,11] A schematic diagram of the spectroscopy system is shown in Fig. 1. The present spectroscopy system comprises four parts: the coherent plasma SXRL, the x-ray image transfer optics using a soft x-ray spherical mirror (SM) for mapping of x-ray source image onto the sample, the Michelson type delay pulse generator, and the picosecond time-resolved x-ray speckle measuring equipment.

A. Coherent soft x-ray source

The coherent x-ray source is a transient electron collision excitation type nickel-like silver SXRL adopted with the double-target configuration.[8,9,12] In order to generate a coherent SXRL pulse, we are using a chirped pulse amplification (CPA) glass laser system.[11,13] The glass laser system consists of an oscillator, an optical parametric CPA (OPCPA) preamplifier, a main amplifier, a pulse compressor, and a pump laser focusing optical system. An infrared seed light at 1053 nm generated by the oscillator is amplified with the OPCPA preamplifier and the main amplifier. This laser system has two output beam lines for x-ray lasing using the double-target configuration, and each beam line produces 20 J IR pump laser beam. The output pump laser beams are focused on a silver slab targets through the pulse compressor and the pump laser focusing optical system, and generate a high-directive, coherent SXRL beam. Characteristics of the double-target SXRL are 13.9 nm in wavelength, 7 ps in pulse width, and 10^{-4} in the bandwidth $\Delta\lambda/\lambda$. The divergence of the SXRL beam is about 0.5 mrad and more than 90% of the SXRL beam is spatially coherent. The coherent photon flux of the SXRL is 3.5×10^{10} photons/pulse.

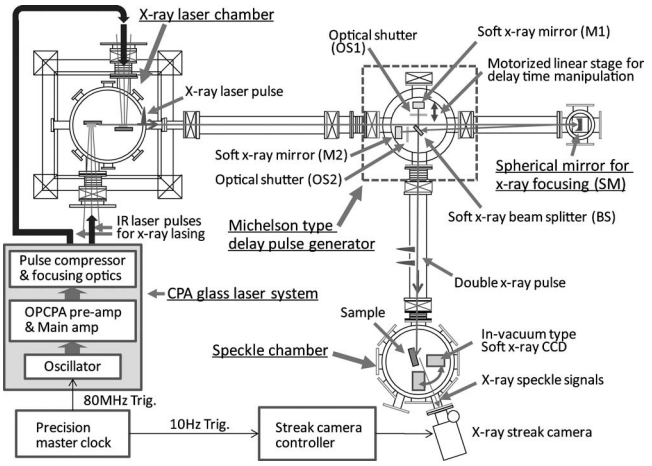

FIG. 1. Schematic diagram of x-ray speckle intensity correlation spectroscopy system using a Michelson type delay pulse generator and a soft x-ray streak camera. M, SM, OS, and BS represent a normal incident Mo/Si multilayer mirror, a normal incident Mo/Si multilayer SM, an optical shutter, and a soft x-ray BS, respectively. All the optical components which compose the present spectroscopy system are set in a vacuum ($\sim 10^{-4}$ Pa) because the wavelength of the x-ray lasing is in the soft x-ray region. The delay time of the second x-ray pulse from the first x-ray pulse can be manipulated by changing the delay path length between the BS and the M1 mounted on the precision motorized linear stage. Driving of the x-ray streak camera is perfectly synchronized with x-ray lasing and x-ray pulse illumination onto the sample by the direct drive technique using the precision master clock.

The SXRL beam is divergent and has a shot-by-shot fluctuation of its pointing within a range of up to 0.5 mrad. Therefore, we have employed the x-ray SM to create an image transfer optical system of the x-ray source. The SM is a Mo/Si multilayer SM optimized for 13.9 nm soft x-ray, having the curvature of 3000 mm and the reflection rate of 70% for 13.9 nm soft x-ray, respectively, and is located 3057 mm downstream of the x-ray source. Because the SM creates an approximately one-to-one mapping of the x-ray image at the x-ray source plasma on the sample surface, the soft x-ray beam is always focused at the same point of the sample surface without its pointing fluctuation. The spot size of the focused x-rays at the sample is approximately 60 μm (full width at half maximum) in diameter.

B. Double pulse and delay generation

In order to generate double coherent SXRL pulses, we have developed a Michelson type delay pulse generator which consists of a soft x-ray beam splitter (BS) and two normal incident soft x-ray Mo/Si multilayer mirrors. In Fig. 2, the photograph of the arrangement of the optical devices is shown. The BS is a multilayer thin film of Mo and Si, fabricated by NTT Advanced Technology Corporation.[14] The BS is optimally designed at an incident angle of 45° for the 13.9 nm x-ray. The transmittance and the reflection rates of the BS at an incident angle of 45° are 30% and 30%, respectively. The x-ray beam from the SM is divided with the BS. The x-rays transmitted through the BS are returned to the BS by the soft x-ray mirror (M2) and part of them is reflected to the sample with the BS. On the other hand, the x-rays reflected by the BS are reflected again by the soft x-ray mirror (M1) and part of them transmits through the

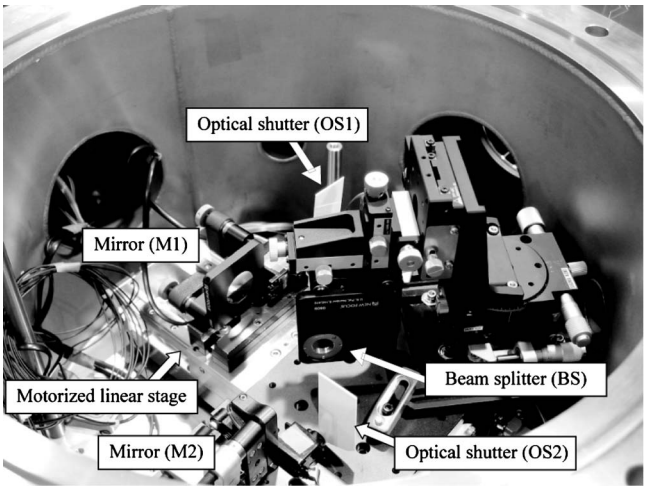

FIG. 2. Photograph of the Michelson type delay pulse generator. The x-ray mirrors are mounted on the motorized mirror mounts, and the motorized optical shutters are placed in front of them. The mirrors and the shutters can be manipulated with a computer. All components are placed in the vacuum chamber.

BS to the sample. The M1 and the M2 are mounted on the motorized optical mounts with actuators (New Focus, Model 8807). Moreover, electric optical shutters (OS1 and OS2) are placed before the M1 and the M2. The M1 is mounted on a precision linear motorized stage (Kohzu Precision Co., Ltd., MVXA10A-L2) and its position can be manipulated by the external motor controller (Kohzu Precision Co., Ltd., SC400). The delay time of the second x-ray pulse from the first x-ray pulse is manipulated by changing the distance between the BS and the M1. The distances from the SM to the BS, from the BS to the M2, and from the BS to the sample are 1057, 75, and 1670 mm, respectively.

C. Time-resolved speckle measuring equipment

The picosecond time-resolved x-ray speckle measuring equipment consists of motorized stages for manipulating the sample position, an in-vacuum soft x-ray charge coupled device (CCD) camera, and a high-speed x-ray streak camera, which are installed in the speckle vacuum chamber. The sample holder having a thermoheater is mounted on the x-z-θ motorized stages (Kohzu Precision Co., Ltd., MVXA10A-L2, ZA10A-W2C, and MVRA07A-W), controlled with the external stage drivers (Kohzu Precision Co., Ltd., SC-400). The sample temperature can be controlled from the room temperature up to 500 K with an accuracy of ± 0.1 K by the thermocontroller (Lakeshore, Model 331 temperature controller). The in-vacuum soft x-ray CCD camera (Roper Scientific, PI-MTE, 13.5 μm^2 pixel size, 2048×2048 pixels) is employed for measuring a speckle pattern due to a single SXRL pulse or for adjusting the focus points of double x-ray pulses on the sample surface. The CCD camera can change its position by the rotation stage around the sample as shown in Fig. 1 to measure the x-rays scattered in various scattering angles. The distance between the sample and the CCD camera is 60 mm.

The soft x-ray streak camera (Hamamatsu Photonics K. K., C4575–01) is used for the time-resolved measurement of

the double x-ray speckles in the range of picoseconds. The photocathode length in it is 11 mm and its fluorescence image caused by x-ray illumination is measured in 672 channels with the digital imaging device of the soft x-ray streak camera. The obtained streak camera image shows the intensity profiles of the x-ray speckles including the specular reflections of the x-ray pulses in the horizontal direction. The distance between the sample and the photocathode of the soft x-ray streak camera is 650 mm. For measuring x-ray speckle signals having tens of picoseconds time-gap, however, the x-ray streak camera needs to be driven within picoseconds of the timing jitter between SXRL illumination onto the sample and its driving. Therefore, we have introduced a precision master clock generator (Tektronix, Inc., DG2040) in the trigger system of the glass laser to diminish the jitter. The master clock generates two trigger signals at 80 MHz and 10 Hz, which are perfectly synchronized. The 80 MHz trigger signal drives the oscillator of the CPA glass laser system and the 10 Hz trigger signal drives the soft x-ray streak camera directly. This technique has enabled to measure the x-ray speckle signals by use of the soft x-ray streak camera within a timing jitter less than a few tens of picoseconds.

III. INTENSITY CORRELATION MEASUREMENTS

It is well known that as a precursor phenomenon near the ferroelectric phase transition temperature Tc of $BaTiO_3$, submicron size ferroelectric ordered small regions,[15] polarization clusters, appear temporarily in paraelectric matrix. Individual polarization that consists of the polarization cluster subjects to the thermal fluctuation[16] with characteristic relaxation time τ_0. For the purpose of the demonstration of the performance of the developed spectroscopy system, we performed soft x-ray speckle intensity correlation experiments for measuring the relaxation time of polarization of the ferroelectric material $BaTiO_3$. Each of the clusters on the $BaTiO_3$ surface near Tc is polarized along one of the crystallographic axes (x, y, z). When the polarized x-ray laser pulse is illuminated on paraelectric $BaTiO_3$ surface near Tc, the polarization clusters linearly polarized in the same direction of the x-ray laser causes phase shift in the x-ray laser waves due to the birefringence, causing the speckle pattern.

The intensity correlation measurements were carried out for various sample temperatures from 393 up to 405 K at delay times of 15, 25, 50, and 110 ps in two different independent experiments. The sample used in the present experiments was flux-grown $BaTiO_3$ single crystal with 395 K in Tc. The SXRL beam is focused onto the (001) surface of $BaTiO_3$ with the gazing angle of 10°.

An example of x-ray streak images of soft x-ray speckles due to the first and the second SXRL pulses and their intensity profiles in the horizontal direction are shown in Fig. 3. The soft x-ray speckle intensity profile consists of two peaks: a large peak around the scattering angle of 0 mrad, which corresponds to the specular reflection of the SXRL pulse, and a small peak around −6 mrad. The appearance of two peaks seems to be due to the surface structure of the sample because their positions are independent from the sample temperature and their intensity ratio changes with the focusing

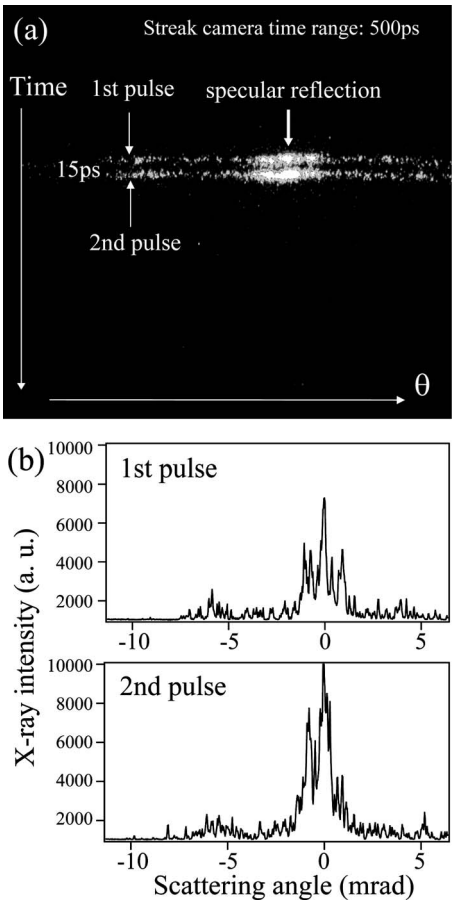

FIG. 3. (a) X-ray streak camera image of x-ray speckles of $BaTiO_3$. (b) The x-ray intensity profiles of them in the horizontal direction. The x-ray streak image shown in Fig. 3(a) was obtained at the sample temperature of 405 K and the delay time of 15 ps. The vertical direction is the time evolution of the speckles and the horizontal direction is the scattering angle θ. The photocathode length of the x-ray streak camera and the pixel number of streak image in the horizontal direction are 11 mm and 672 channels, respectively. The parallel direction of Fig. 3(b) is the scattering angle.

position of the SXRL pulse on the sample surface. The widths of the speckles visible in Fig. 3(b) are consistent with the speckle size 0.276 mrad estimated from the inverse size of the illuminated region. The intensity correlation analysis was carried out for the specular reflection peak data on the right side. The number of x-ray laser shots to calculate each of the intensity correlations at various sample temperatures and pulse delay times was from seven to ten shots.

First of all, we normalized each intensity profile by sum of signal magnitudes at all channels in order to cancel the shot-by-shot fluctuation of the SXRL intensity. And then we calculated the intensity correlations expressed by the following equation from the normalized x-ray speckle intensity distribution data at the various sample temperatures:

$$g^{(2)}(\tau) = \frac{\langle I(t+\tau)I(t)\rangle_t}{\langle I(t)\rangle_t^2}, \quad (1)$$

where τ is the delay time of the second SXRL pulse from the first one. Here, the intensity correlation $g^{(2)}$ on thermal fluctuation of the dipole moment in the polarization cluster can be expressed by the following exponential type function having a relaxation time τ_0 (Ref. 17)

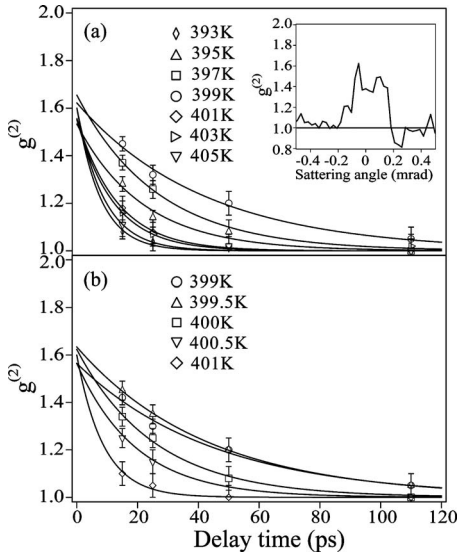

FIG. 4. Decay curves of $g^{(2)}$ as a function of delay time at several sample temperatures from 2 K below Tc up to 10 K above Tc (Tc=395 K). (a) and (b) were independently obtained in the first experiment and in the second experiment, respectively. The inset of Fig. 4(a) shows the $g^{(2)}$ profile around the specular reflection signal obtained at the sample temperature of 399 K and the delay time of 15 ps. The solid lines are the fitting results with the Eq. (2) by means of the least-square method.

$$g^{(2)}(\tau) = 1 + \beta \exp\left(-\frac{2\tau}{\tau_0}\right), \tag{2}$$

where β is a parameter related to the visibility of x-ray source. We evaluated τ_0 by the curve fitting of the calculated $g^{(2)}$ data to Eq. (2) by use of the least-square method. The results are shown in Fig. 4. Figures 4(a) and 4(b) show the relaxation behavior at the temperatures from 393 up to 405 K by 2 K obtained in the first experiment and at the temperatures from 401 up to 405 K by 0.5 K obtained in the second experiment, respectively. Moreover, the $g^{(2)}$ profile in the region of the specular reflection signal corresponding to the divergence of the SXRL (~0.5 mrad) at the sample temperature of 399 K is shown in the inset of Fig. 4(a). The $g^{(2)}$ values on the outside of the specular signal region wildly fluctuate around $g^{(2)}=1$ because of the poor signal to noise ratio of the x-ray speckle signal, so that we do not discuss the $g^{(2)}$ values in that region here.

In Fig. 4, the values of $g^{(2)}$ calculated from the intensity data of specular reflection fit well to the exponential decay type function expressed by Eq. (2). Moreover, the intercepts at $\tau=0$ for all the sample temperatures, namely, β in Eq. (2), must be almost same value because it depends on only the visibility of the x-ray source. As shown in Fig. 4, they are around 0.6 for all sample temperatures. Agreement in the β values for all sample temperature and the coincidence in the τ_0 at 399 and 401 K in Figs. 4(a) and 4(b) confirm the reproducibility of the present experiments.

IV. DISCUSSION

As shown in the inset in Fig. 4, $g^{(2)}$ has large values in the region of the x-ray scattering angle of about 0.24 mrad in the vicinity of the center of the specular reflection peak. The obtained scattering angle of 0.24 mrad corresponds to the speckle size determined by the spot size of the incident SXRL pulse on the sample surface and the scattering wave in this region is spatially coherent. Intensity correlation within the center parts of the specular reflection reflects the correlation among the coherent scattering amplitudes by the polarization in clusters. Time correlation of specular reflection intensities exhibits the time evolution of the decay of the spatial correlation of polarizations of the same points.

The relaxation times estimated from the experimentally obtained speckles are in the range of several tens of picoseconds, which is consistent with the value estimated from the central peak observed in Fabry–Pérot spectrum.[16] Moreover, $\beta=0.6$ obtained by the present experiments corresponds to the visibility of 0.8. Considering the SXRL beam divergence of 0.5 mrad for the present experiments, the value of the visibility 0.8 is consistent with the value of the visibility 0.98 estimated by the Young's double-slit interference experiment with the SXRL of which the beam divergence was 0.2 mrad.[9] Large values in visibility due to the high coherence of the plasma SXRL confirm the high signal to noise ratio of the present method even in picosecond region.

V. CONCLUSION

We have developed the soft x-ray speckle intensity correlation spectroscopy system using the picosecond single shot coherent x-ray laser capable of directly probing the dynamic behavior of materials on the picosecond time scale. We confirmed the capability of the system by observing the relaxation time of the polarizations in polarization clusters in paraelectric $BaTiO_3$ in the vicinity of Tc. Detail of the physics of the present observation has been presented elsewhere.[17] The present intensity correlation spectroscopy system is widely applicable to other materials such as charge density wave, spin density wave, and high Tc superconductor as well as ferroelectric material. Moreover, this method is applicable to x-ray photon correlation spectroscopy of single shot x-ray source such as x-ray free electron laser.

[1] M. Sutton, S. G. J. Mochrie, T. Greytak, S. E. Nagler, L. E. Bermann, G. A. Held, and G. B. Stephenson, Nature (London) **352**, 608 (1991).
[2] A. Fluerasu, M. Sutton, and E. M. Dufresne, Phys. Rev. Lett. **94**, 055501 (2005).
[3] A. Robert, J. Wangner, T. Autenrieth, W. Hartl, and G. Grubel, J. Magn. Magn. Mater. **289**, 47 (2005).
[4] L. M. Stadler, B. Sepiol, B. Pfau, G. Vogl, and F. Zontone, Nucl. Instrum. Methods Phys. Res. B **238**, 189 (2005).
[5] O. G. Shpyrko, E. D. Isaacs, J. M. Logan, Y. Feng, G. Aeppli, R. Jaramillo, H. C. Kim, T. F. Rosenbaum, P. Zschack, M. Sprung, S. Narayanan, and A. R. Sandy, Nature (London) **447**, 68 (2007).
[6] S. Brauer, G. B. Stephenson, M. Sutton, R. Bruning, E. Dufresne, S. G. J. Mochrie, G. Grubel, J. Als-Nielsen, and D. L. Abernathy, Phys. Rev. Lett. **74**, 2010 (1995).
[7] S. B. Dierker, R. Pindak, R. M. Fleming, I. K. Robinson, and L. Berman, Phys. Rev. Lett. **75**, 449 (1995).
[8] M. Tanaka, M. Nishikino, T. Kawachi, N. Hasegawa, M. Kado, M. Kishimoto, K. Nagashima, and Y. Kato, Opt. Lett. **28**, 1680 (2003).
[9] M. Nishikino, M. Tanaka, K. Nagashima, M. Kishimoto, M. Kado, T. Kawachi, K. Sukegawa, Y. Ochi, N. Hasegawa, and Y. Kato, Phys. Rev. A **68**, 061802(R) (2003).
[10] T. Kawachi, K. Nagashima, M. Kishimoto, N. Hasegawa, M. Tanaka, Y. Ochi, M. Nishikino, H. Kawazome, R. Z. Tai, K. Namikawa, and Y. Kato, Proc. SPIE **5919**, 59190L (2005).

[11] M. Kishimoto, K. Nagashima, T. Kawachi, N. Hasegawa, M. Tanaka, Y. Ochi, M. Nishikino, K. Sukegawa, H. Yamatani, Y. Kunieda, S. Namba, K. Namikawa, and Y. Kato, Proc. SPIE **6702**, 67020P (2007).
[12] T. Kawachi, M. Kado, M. Tanaka, A. Sasaki, N. Hasegawa, A. V. Kilpio, S. Namba, K. Nagashima, P. Lu, K. Takahashi, H. Tang, R. Tai, M. Kishimoto, M. Koike, H. Daido, and Y. Kato, Phys. Rev. A **66**, 033815 (2002).
[13] T. Kawachi, M. Kado, M. Tanaka, N. Hasegawa, K. Nagashima, K. Sukegawa, P. Lu, K. Takahashi, S. Namba, M. Koike, A. Nagashima, and Y. Kato, Appl. Opt. **42**, 2198 (2003).
[14] H. Takenaka, S. Ichimaru, T. Haga, T. Ohchi, H. Ito, Y. Muramatsu, E. M. Gullikson, and R. C. C. Perera, J. Phys. IV **104**, 251 (2003).
[15] R. Z. Tai, K. Namikawa, A. Sawada, M. Kishimoto, M. Tanaka, P. Lu, K. Nagashima, H. Maruyama, and M. Ando, Phys. Rev. Lett. **93**, 087601 (2004).
[16] J. P. Sokoloff, L. L. Chase, and D. Rytz, Phys. Rev. B **38**, 597 (1988).
[17] K. Namikawa, M. Kishimoto, K. Nasu, E. Matsushita, R. Z. Tai, K. Sukegawa, H. Yamatani, N. Hasegawa, M. Nishikino, M. Tanaka, and K. Nagashima, Phys. Rev. Lett. **103**, 197401 (2009).